Hybrid supercapacitor based on poly(aniline-co-m-anilicacid) and activated carbon in non-aqueous electrolyte

Muthu Selvakumar*,† and Sethuraman Pitchumani**

*Department of Chemistry, Manipal Institute of Technology, Manipal 576104, India
**Central Electrochemical Research Institute, Karaikudi 630006, India

Abstract−A hybrid asymmetrical super capacitor has been fabricated based on p-doped poly(aniline-co-m-anilicacid) and activated carbon coated on SS electrodes. The characterization of material, electrode and performance of the super capacitor has been studied by FTIR, Cyclic Voltammetry, TGA/DTA, AC Impedance spectroscopy, and galvanostatic charge-discharge tests. The super capacitor showed a maximum specific capacitance of 102 F/g at a scan rate of 10 mV/s. The normalized active-reactive power behavior of the capacitor has been determined. The time constant calculated for the super capacitor is 6 milliseconds, indicating the suitability of the system for efficient use at low frequency range.

Key words: Supercapacitor, Hybrid Supercapacitor, Conducting Polymer, Activated Carbon, Doping, Capacitance, Poly (aniline-co-m-anilicacid)

INTRODUCTION

The potential applications of conducting polymers include cathode materials for lithium batteries [1], their applications in polymer light emitting diodes [2], molecular electronic devices [3], conducting fibers [4] and electrochemical capacitors [5]. In contrast to other conducting polymers such as polythiophene, polypyrrole and polyaniline have good environmental stability and redox properties associated with chain nitrogen. Theoretical studies on n-doping and p-doping of polyaniline are well-documented in the literature [6], and the first successful chemical n-doping of polyaniline has also been reported by Hua et al. [7]. But for n-doped at less negative potentials, higher doping level values are required for materials with almost the same specific capacitance due to the high molecular weight monomer unit [8,9]. This is a defect of conducting polymer-based electrochemical capacitors because the need for very high doping levels concomitantly requires insertion/de-insertion of counter ions that cause a volume change of the polymer. It is important to have electro active polymers such as polyaniline and its derivatives to maintain its conductivity at a pH value greater than 4, but the conductivity of polyaniline falls down in non-aqueous electrolyte (less acidic pH). To overcome this drawback, an attempt has been made to synthesize poly(aniline-co-m-anilicacid) that remains conductive in lesser pH. The introduction of sulphonic acid group as a substitutent does not allow the conductivity to fall drastically with increase in pH as it happens with polyaniline [10]. Thus, realizing the problem of adapting polyaniline to neutral pH, an alternative approach has been made through substituted (self doped) polyaniline. The substituents are from electron-donating groups such as alkyl groups [10,11], alkoxy [12,13] and electron withdrawing groups, namely chloro and nitro groups [14,15]. But these attempts have resulted

in lowering the conductivity of conducting polymers. To realize a polymer with higher conductivity, at both low pH and high pH, monomers such as m-anilicacid have been incorporated into aniline moiety and poly(aniline-co-m-anilicacid) copolymer formed. This copolymer capable of undergoing redox transformation has been successfully trapped. The capacitance value is much higher compared to that of Kwang Sun Ryu et al. [16], because double layer and pseudo capacitance are involved in this case. In this study, an investigation is made on performance of a hybrid asymmetric supercapacitor which has electronically conducting p-doped poly(aniline-co-m-anilicacid) acting as the positive electrode material, and activated carbon (AC) with high specific surface-area as the negative electrode material instead of n-dopable conducting polymers; the idea already worked for Park and Park [17]. But they were working on aqueous electrolyte up to 1.4 V. A specific capacitance calculated under 4,000 cycles of 380 Fg^{-1} is obtained; here in this work care is taken of the effort of non-aqueous electrolyte and reaches the maximum voltage 2.4 V. Towards this, p-type electrodes are characterized through FTIR, UV and cyclic voltammetry techniques for supercapacitor application. From AC impedance spectroscopy study the active region of hybrid electrochemical capacitors based on poly(aniline-co-m-anilicacid) and activated carbon electrode was figured out. In the present study, poly(aniline-co-m-anilicacid) was chemically synthesized and used for active materials for asymmetric electrochemical supercapacitors. The performance of the so fabricated supercapacitor has been studied by cyclic voltammetry, AC Impedance spectroscopy and galvanostatic charge-discharge with AUTOLAB 30.

EXPERIMENTAL

1. Reagents

Aniline (GR-Merck) (distilled before use), HBF₄ (GR-Merck) Polyvinyledenefluoride (Aldrich) n-methylpyroldine (Aldrich), m-Anilicacid (GR-Merck) were used as received. All the experimental

---

†To whom correspondence should be addressed.
E-mail: chemselva78@gmail.com

preparation was carried out using Millipore water (Milli-Q water purification system).

2. Preparation of Poly(aniline-co-m-anilicacid)

Monomer solution was prepared by dissolving the 0.25 g of m-anilic acid in 30 ml of 1 M HBF₄ and to this resultant solution; 1 ml of aniline was added and kept in an ice bath [0 °C to 4 °C] for up to four hours. 1.15 g of $(NH_4)_2S_2O_8$ dissolved in 10 ml of water, was added to the prepared monomer solution, and kept in the ice bath (0 °C to 4 °C) for four hours. The resultant colored precipitate was collected and washed in triple distilled water and dried.

3. Spectroscopy Characterization of Copolymer

The chemically synthesized copolymer namely poly(aniline-co-m-anlicacid) has been characterized using FTIR, TGA/DTA and UV. FTIR measurements were conducted using a Nex vs 670 FTIR spectrometer with DTGS detector. The FTIR study spectrum was taken in the mid IR region of 400-4,000 cm⁻¹ with 16-scan speed. The samples were mixed with spectroscopically pure KBr in the ratio of 1 : 100; pellets were fixed in the sample holder while the analyses were carried out. UV measurements were conducted using Varian Cary 500 UV spectroscopy.

4. Electrochemical Characterization Techniques

The capacitor performance was characterized by means of cyclic voltammetry using an AUTOLAB from Eco-Chemie; AC impedance measurements were made in the frequency range of 0.01 Hz to 10^6 Hz. The charge-discharge behavior of the fabricated super capacitor was tested by using the galvanostatic method. A three electrode system was employed with saturated KCL for p-doping used as a reference electrode, Pt as a counter electrode and stainless steel (304 qualities, 1 cm×2 cm×0.2 mm) pasted by poly(aniline-co-m-anilicacid) act as a working electrode.

5. Preparation of the Electrode

Poly(aniline-co-m-anilicacid) and activated carbon (Aldrich) was made into a paste by using N-methylpyrrolidine along with a binder, polyvinylidiende fluoride, in the ratio of 70 : 30 using a pestle and mortar. This paste was then applied with a brush to a pre-weighed stainless steel current collector and dried at room temperature.

RESULTS AND DISCUSSION

1. Cyclic Voltammetry, FTIR and UV Spectroscopy

The chemically synthesized poly(aniline-co-m-anilicacid) pasted on SS electrodes was carried out by cyclic voltammetry with 1 cm² SS electrodes in the electrolyte containing 0.1 M HBF₄. In all of the electrochemical studies voltammetric scans were terminated at the positive potential limit to ensure that within 500 cycles the electrodes were doped sufficiently. Anionic doping or p-doping is a phenomenon wherein the oxidation caused by a chemical species generates a positively charged conducting polymer with an associated anion, as depicted below which is relevant to the present study.

$$PANI + n \, HBF_4 \rightleftharpoons P \, [ANI]^{n+} \, [BF_4^-]_n^{n-} + nye^-$$
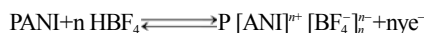
For p-doping the electrode, cyclings (500 cycles) were done at a scan rate of 50 mV/sec by keeping the potential between −0.2 V to +0.8 V. Fig. 1 shows the cyclic voltammogram (CV) for the electrodeposition p-doped poly(aniline-co-m-anilicacid) film on the SS electrode in monomer-free solution at 500th cycle as well as 50 and 200th cycle, fig also presented. The current increased from 50 to 200
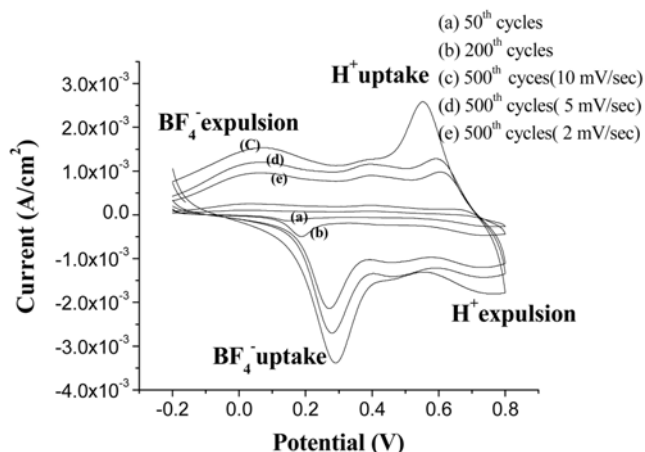
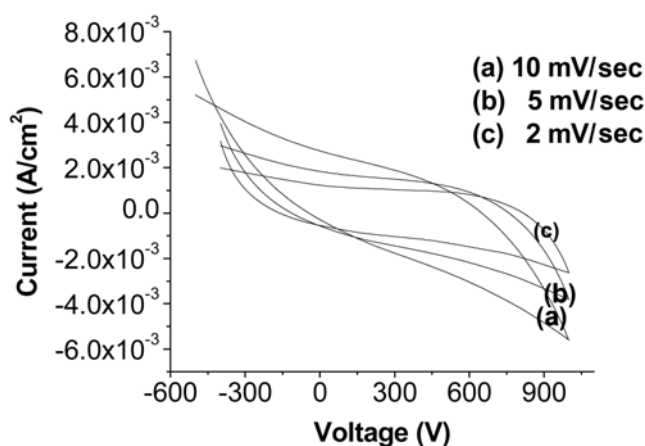**Fig. 1. CVs of P doping cycling in 0.1 M HBF₄ at different scan rate.**

Fig. 2. CVs of activated carbon in $(C_2H_5)_4NH_4BF_4$ at different scan rate.

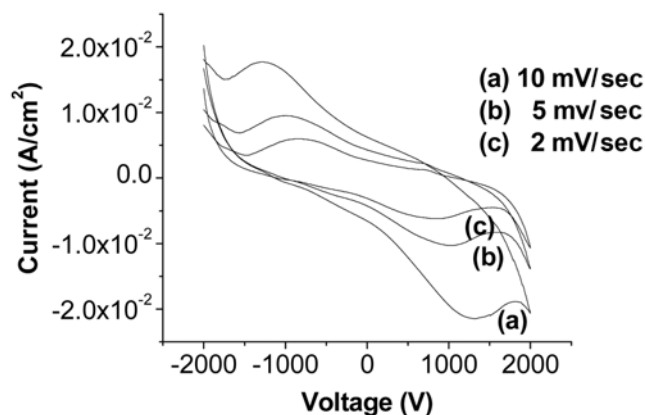**Fig. 3. CV of hybrid supercapacitor in 0.1 M $(C_2H_5)_4NH_4BF_4$ at different scan rate.**

cycles and reached a maximum at 500 cycles, ensuring the formation. The CV shape for the PANI electrode resembles that for electroactive polyaniline (co-m-anilicacid) in neutral aqueous solution [18]. Cyclic voltammogramms for the activated carbon pasted electrodes at various potential sweep rates are shown in Fig. 2. For the
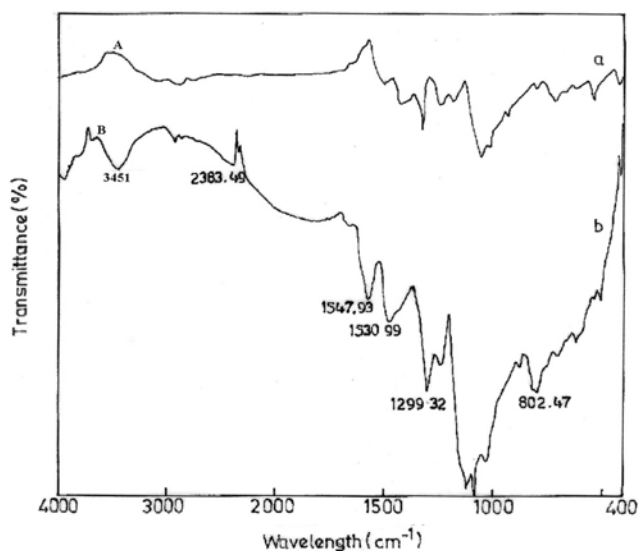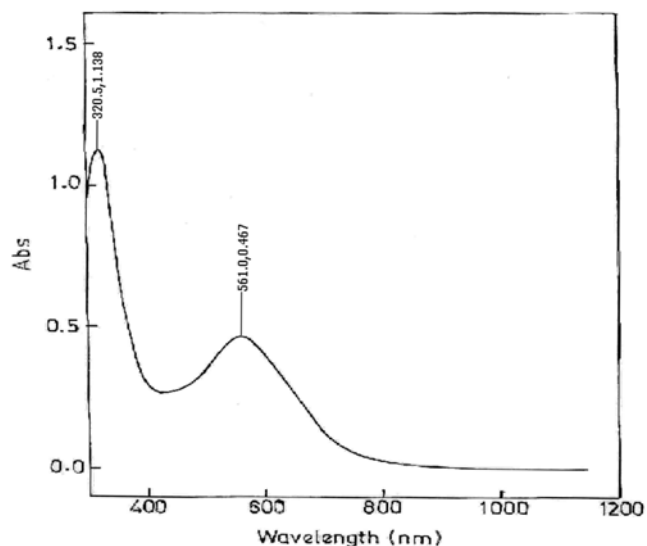
Table 1. Specific capacitance for the materials

Type	Material	Active material (gm)	Scan rate (mV/Sec)	C (F/g^{-1})
p-Type	Poly(aniline-co-m-anilicacid)	0.0030	10	137
			5	125
			2	67
n-Type	Activated carbon	0.0030	10	44
			5	22
			2	12
Hybrid super capacitor	Both	0.0030	10	102
			5	88
			2	72

activated carbon based electrodes, nearly rectangular CV curves are obtained due to a charge separation with the same magnitude between the electrode-electrolyte interfaces [17]. The cyclic voltammogram of hybrid supercapacior in 0.1 M Tetraethyl ammonium tetrafluoborate in acetonitrile is shown in Fig. 3, which indicates a good capacitive behavior. The behavior observed is characteristic of double layer (activated carbon), redox poly(aniline-co-m-anilicacid), and a perfect synchronization of double layer and redox (hybrid supercapacitor) capacitive features. The specific capacitance values of the p-doped electrode at 500th cycles, activated carbon electrodes and the super capacitor for the different scan rate (Table 1) have been calculated from the respective cyclic voltammograms using the equation:

$$C = \frac{i}{s}$$

Where s is the potential sweep rate and i is the average current. The specific capacitance increase by more than three times compared with that of a symmetric PANI, asymmetric PANI-based capacitor using an aqueous acid electrolyte, or a non-aqueous electrolyte [19, 20]. In addition, the specific capacitance of the poly(aniline-co-m-anilicacid)-activated carbon, non-aqueous base hybrid type EC capac-


Fig. 5. UV spectra of poly(aniline-co-m-anilicacid).

itor shows similar or higher values than those reported for poly(3-methyl thiophene), poly(ethylenedioxythiophene) based EC capacitor [21,22].

Further FTIR of undoped and p-doped electrode were taken to confirm the doping (Fig. 4). From the figure it can be seen that doping induced bands originating from changes in the conjugated backbone due to the electron withdrawing and electron donating dopants on the polymer chain and counter ion balancing appears at 3,451, 1,530, and 1,547, 1,090 and 802 cm^{-1} [23,24]. To substantiate the conformation of copolymer and doping, UV spectroscopy was taken and evaluated. From Fig. 5, the observed peak at 320 nm is attributed to π-π^* transition in benzenoid units that refers to polaron. The second peak at 560 nm is attributed to an exciton transition and it refers to a bipolaron [25]. The quinoid form of diamino units, which is in conducting form, is responsible for the conductivity in copolymers.

2. Thermal Analysis of Poly(aniline-co-m-anilicacid)

The general trends in the weight losses are well understood. However, thermal gravimetric analysis was carried out on chemically prepared poly(aniline-co-m-anilicacid). Thus, it is possible to correlate the observed changes in electro activity with the known physi-

Fig. 4. FTIR spectra of undoped and p doped poly(aniline-co-m-anilicacid).
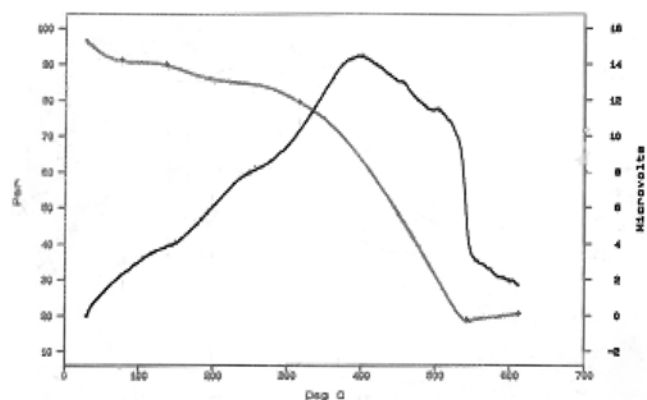
Fig. 6. TGA/DTA for poly(aniline-co-m-anilicacid).

cal/chemical changes in polymer structure and morphology that thermal treatment induces. Poly(aniline-co-m-anilicacid) powder prepared after chemical oxidation and in the doped state with HBF_4 showed good thermal stability under nitrogen; as seen in (Fig. 6) the t.g.a trace is consistent with what has been published previously in the literature [26]. Continuous weight loss was observed above room temperature, although this may be broken down into three steps. Up to a temperature of 200 °C, 18% of the polymer weight was lost. This may be attributed to evaporation of moisture and HBF_4 and probably some low-molecular-weight polymer segments as well as trapped F_2 formed during chemical oxidation [27]. The d.t.a curve shows a negative change for this weight loss, indicating an endothermic heat associated with it, which is consistent with the attributed physical changes. The loss between 200 and 400 °C corresponded with decrease in elctroactivity observed above after such treatment. The major mass loss was observed at 380 °C. The total weight loss was due to polymer backbone degradation. Here the d.t.a. curve shows a large exothermic change consistent with a chemical degradation reaction. It has been shown that under these condi-

tions at temperatures above 150 °C elimination of the dopant (HBF_4) on the amino group occurs simultaneously with chlorination of the polymer's aromatic rings [28].

2-1. AC Impedance Spectroscopy

The AC impedance responses of the individual undoped, p-doped and activated carbon electrodes in monomer free solution are shown in Figs. 7 and 8. As is evident from the figures, the formation of semicircles is observed at high frequencies in the range 1 MHz to 10 KHz and an almost a straight line in the low frequency region. The capacitance value of the electrodes increased at low frequencies due to a larger number of ions movement, which caused a decrease in the bulk resistance of the capacitor. The semi-circle results from the parallel combination of resistance and capacitance and the linear region is due to Warburg impedance [29]. At low frequency region, the linear part leans more towards the imaginary axis, indicating a good capacitive behavior. The Nyquist plot of the hybrid supercapacitor (Fig. 9) also shows the similar behavior. The capacitance, internal resistance and time constant are of importance for considering the capacitor performance. Supercapacitors gener-
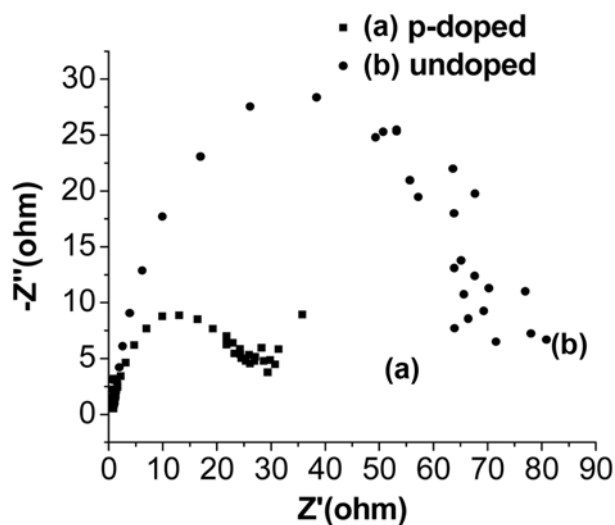

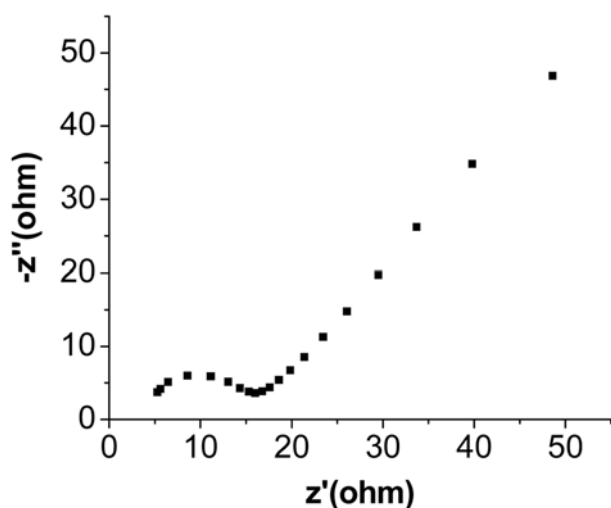Fig. 7. Nyquist plot of undoped and p-doped electrode.

Fig. 9. Nyquist plot of hybrid supercapacitor.
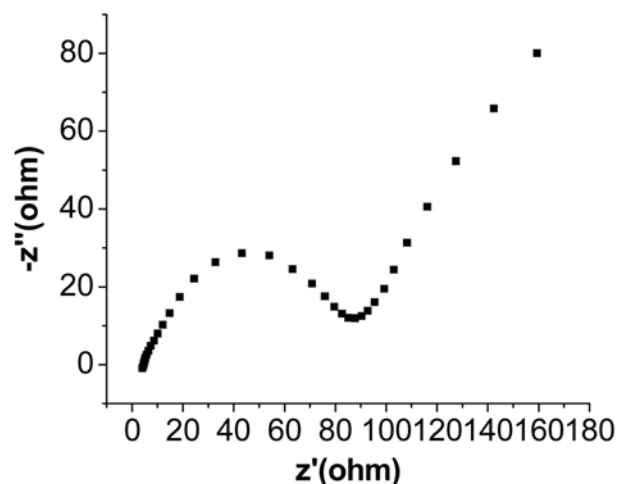

Fig. 8. Nyquist plot of activated carbon.

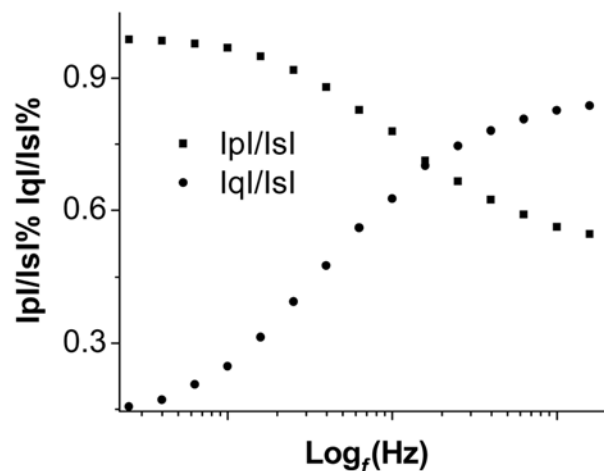Fig. 10. Normalized reactive power |Q|/|S|% and active power |P|/|S|% vs. frequency (Hz). Plot for the 1 cm² cell for hybrid-supercapacitor.
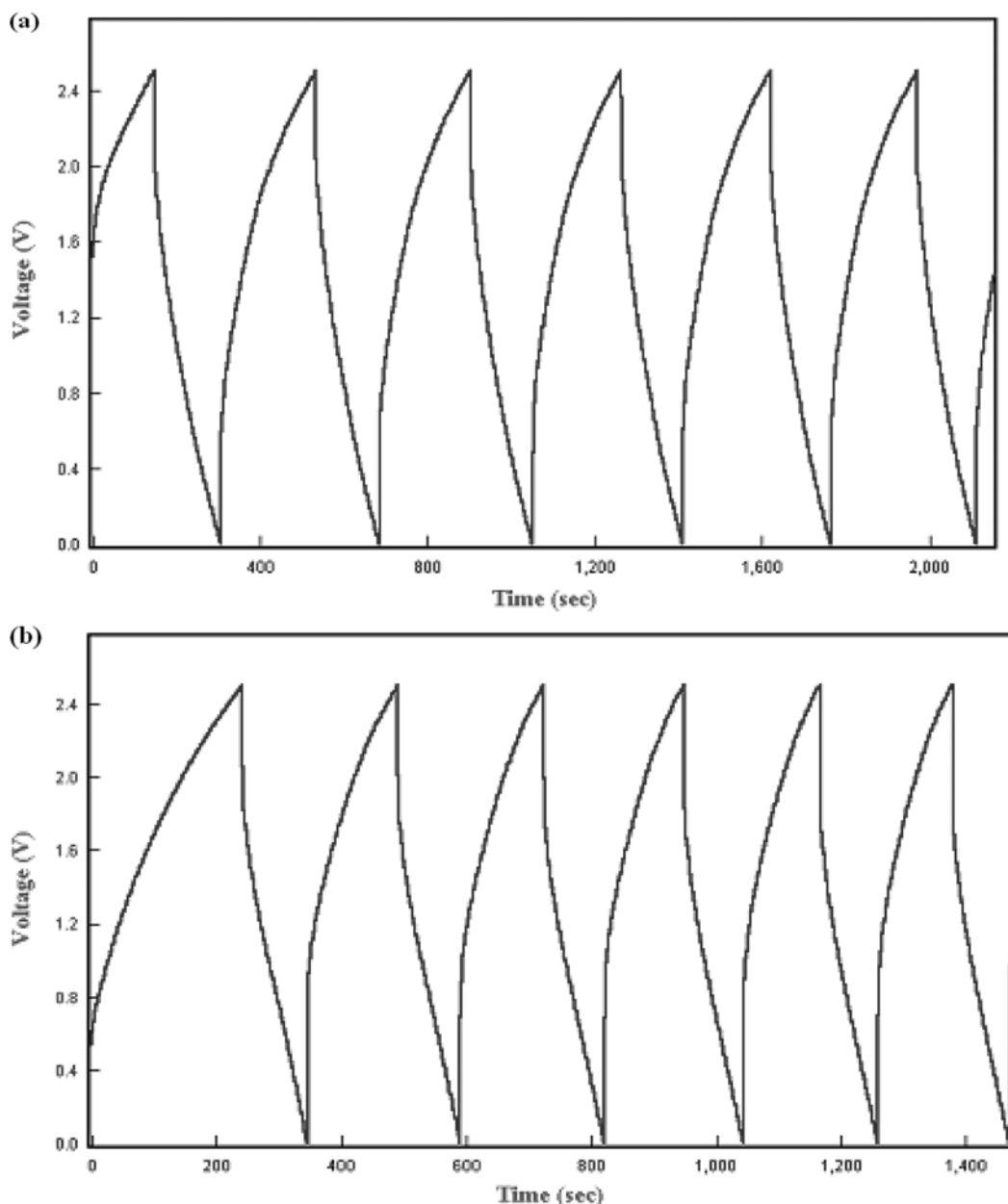
Fig. 11. Galvanostatic charge-discharge curves of hybridsupercapacitor at different current density (a) 2 mA (b) 3 mA.

ally oscillate between two states: resistive at high frequencies and capacitative at low frequencies. Between these two states they behave like a resistance capacitance transmission line circuit [30,33]. At high frequencies, supercapacitors behave like a resistance. At low frequency, the imaginary part of the impedance sharply increases and the plot tends to a vertical line characteristic of capacitive behavior. In the middle frequency range, the influence of electrode porosity and thickness on the migration rates of ions from the electrolyte inside the electrode can be seen [14]. This shifts the low frequency capacitive behavior along the real axis toward more resistive values. Fig. 12 presents the normalized reactive power, $|Q|/|S|$ and active power $|P|/|S|$ versus frequency plot for the super capacitor. The theoretical details of this plotting technique can be found elsewhere [13]. This plot provides information regarding the difference in the way to change from resistive to capacitive behavior of

the system. The change occurs roughly from 5 KHz (resistive) down to 50 Hz (capacitive), i.e., over three orders of magnitude. Hence, use of this capacitor can be achieved with high efficiency at comparatively low frequencies only. The plot also enables the calculation of time constant, also known as dielectric relaxation time, τ_o. The time constant for the solid state capacitor under study was calculated to be 6.0×10^{-2} second. The time constant τ_o, represents [13] a transition for the super capacitor between a resistive behavior for frequency higher than $1/\tau_o$ and a capacitive behavior for frequencies lower than $1/\tau_o$, indicating that the present system can be efficiently used up to 15 Hz.

2-2. Charge - Discharge Characterization

The conducting polymers used in type III capacitors are p- and n-doped as the positive and the negative electrodes, respectively. When the capacitor is charged, the positive electrode is fully p-doped
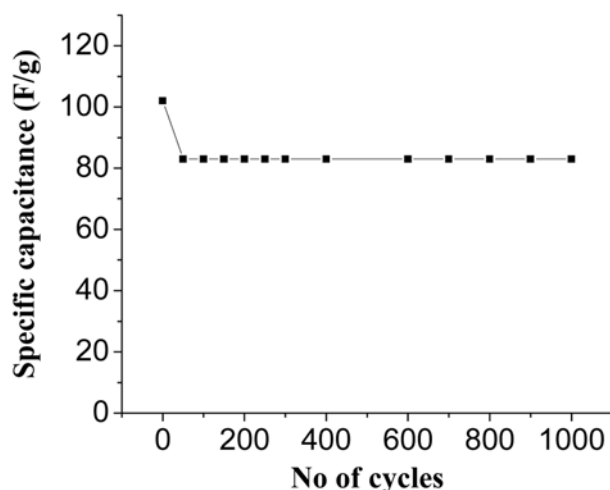
Fig. 12. Specific capacitance vs number of cycles.

and the activated carbon is fully n-doped. The p- and n-doping sources come from the electrolyte, such as cations of Bu_4N^+ and anions of BF_4^-. These doping charges are released on discharge [34]. When the cell is fully discharged, both electrodes end up in their undoped state. Fig. 11 presents the charge-discharge of the hybrid supercapacitor depicting its charge-discharge characteristics at various current density 2 mA, 3 mA. The specific power, specific energy and columbic efficiencies of the supercapacitor are $0.34 \, Wg^{-1}$, $34.33 \, Whg^{-1}$ and 85%, respectively. The specific capacitance calculated under cyclings is 1st 500th and $1{,}000^{th}$ cycle for 102, 83 and 83 Fg^{-1}, indicating almost negligible decrease in the capacitance under cyclings. Fig. 12 presents the variation of specific capacitance of the supercapacitor with cyclings. The data reflects that the device exhibited almost constant capacitance during the test.

CONCLUSION

A hybrid supercapacitor based on p-doped poly(aniline-co-m-anilicacid) and activated carbon has been fabricated and studied for the first time in non-aqueous electrolyte up to 1,000 cycles. The performance evaluation study reveals that p-doped and activated carbon electrodes can be successfully prepared and are suitable for the fabrication of a supercapacitor. The supercapacitor can be used efficiently at low frequency range up to 15 Hz. Efforts are being made to improve the performance of the supercapacitor.

ACKNOWLEDGMENTS

REFERENCES

1. P. Croce, S. Passerini and B. Scrosati, *J. Electrochem. Soc.*, **141**, 1405 (1994).
2. J. Osaka, S. Komaba, N. Fujihana, J. Momma and N. T. Laneco, *J. Electrochem. Soc.*, **144**, 742 (1997).
3. G. P. Kitteson, H. S. White and M. S. Wrighton, *J. Am. Chem. Soc.*, **106,** 7389 (1984).
4. B. R. Mattes, H. Wang, D. Yang, Y. T. Zhu, W. R. Blamenthal and M. F. Hundley, *Synth. Met.*, **45**, 84 (1997).
5. A. Rudge, J. Davey, J. Raistrick and S. Gottesteid, *J. Power Sources*, **47**, 89 (1994).
6. J. Libent, J. W. Bredas and A. J. Esptein, *Phys. Rev. B.*, **51**, 5711 (1995).
7. M. Y. Hua, G. W. Hwang, Y. H. Chuang, S. A. Chen and R. Y. Tsai, *Macromolecules*, **33**, 6235 (2000).
8. A. A. Karyakin, A. K. Strakhova and A. K. Yatsimirsky, *J. Electroanal. Chem.*, **259**, 371 (1994).
9. W. Shenglong, W. Fosong and G. Xiabhui, *Synth. Met.*, **16**, 99 (1998).
10. M. Leclerc, J. Guay and L. H. Dao, *J. Electroanal. Chem.*, **21**, 251 (1988).
11. D. Macinnes and B. L. Funt, *Synth. Met.*, **25**, 235 (1998).
12. W. A. T. Gazotti, J. Matecio and M. A. Depaoli, *Electrochim. Acta*, **43**, 457 (1998).
13. X. H. Wang, L. X. Wang, X. P. Jing and F. S. Wang, *Synth. Met.*, **69**, 335 (1995).
14. M. Ranger and M. Leclerc, *Synth. Met.*, **84**, 85 (1997).
15. M. A. Christopher and C. Brett Thiemann, *J. Electroanal. Chem.*, **538**, 215 (2002).
16. K. Ryu, K. Kim, N. Park, Y. Park and S. Chang, *J. Power Sources*, **103**, 305 (2002).
17. J. H. Park and O. Park, *J. Power Sources*, **111**, 185 (2002).
18. D. W. Hatchett, N. Jsowicz and J. Janata, *J. Electrochem. Soc.*, **146**, 4535 (1999).
19. K. S. Ryu, K. M. Kim, N.-G. Park, Y. J. Park and S. H. Chang, *J. Power Sources*, **103**, 305 (2002).
20. A. Clemete, S. Panero, E. Spila and B. Scrosati, *Solid State Ionics*, **85**, 273 (1996).
21. C. Arbizzani, M. Mastragostino and F. Soavi, *J. Power Sources*, **100**, 164 (2001).
22. K. S. Ryu, Y.-G. Lee, Y.-S. Hong, Y. J. Park, X. Wu, K. M. Kim, M. G. Kang, N.-G. Park and S. H. Chang, *Electrochim. Acta*, **50**, 843 (2004).
23. K. I. Seo and I. J. Chung, *Polym.*, **41**, 4491 (2004).
24. F. Tranvan, S. Garreau, G. Louarn, G. Froyer and C. Chevrot, *J. Mater Chem.*, **11**, 1378 (2001).
25. D. W. Hatchett, M. Jsowicz and J. Janata, *J. Electrochem. Soc.*, **146**(12), 4535 (1999).
26. Y. Wei and K. F. Hsueh, *J. Polym. Sci.*, **27**, 4351 (1989).
27. R. Ansari, W. E. Price and G. G. Wallace, *React. Funct. Polym.*, **56**, 141 (2003).
28. T. Hagiwara, M. Yamaura and K. Iwata, *Synth. Met.*, **25**, 243 (1988).
29. B. E. Conway, Electrochemical Supercapacitors: Scientific Fundamentals and Technological Applications, Kluwer Academic Publishers, Plenum press, New York (1999).
30. D. Qu and H. Shi, *J. Power Sources*, **74**, 99 (1998).
31. H. K. Song, Y. H. Jung, K. H. Lee and L. H. Dao, *Electrochim. Acta*, **44**, 3513 (1999).
32. H. Keiser, K. D. Beccu and M. A. Gutjahr, *Electrochim Acta*, **12**, 539 (1976).
33. P. L. Taberna, P. Simon and J. F. Fauvarque, *J. Electrochem. Soc.*, **150**(3), A292 (2003).
34. J. P. Zheng, J. Huang and T. R. Jow, *J. Electrochem. Soc.*, **144**(6), 2026 (1997).